Large-eddy simulation on staggered grids using the stretched-vortex subgrid model

T. W. Mattner

School of Mathematical Sciences
The University of Adelaide, South Australia 5005, Australia

Abstract

The aim of this work is to develop and test tuned finite-difference and interpolation schemes for large-eddy simulation of incompressible turbulent flows on staggered grids using the stretched-vortex subgrid model. Results from large-eddy simulations of isotropic homogeneous turbulence confirm that standard explicit schemes have a significant effect on resolved-scale statistics, whereas the tuned schemes tend to produce more self-consistent results.

Introduction

A large-eddy simulation (LES) is a numerical simulation of a turbulent flow using a grid that is too coarse to resolve the full range of spatial scales. Such simulations are useful when it would be computationally impracticable to resolve the full range of scales, as is typically the case for high Reynolds number flows. The effects of the unresolved subgrid scales must be accounted for by means of a subgrid model and this involves a certain degree of approximation. Many such models have been proposed. In this study, we focus on the stretched-vortex model developed by Pullin and coworkers [7, 11, 10, 3, 1, 2].

Staggered grids are often used in the simulation of incompressible flows because they help to avoid unphysical pressure oscillations and have good discrete conservation properties [8]. These properties are especially desirable for large-eddy simulations of incompressible flows. On a collocated grid, pressure oscillations are often controlled by numerical schemes that introduce artificial energy dissipation. Dissipative numerical schemes have the potential to overwhelm subgrid models, as is observed in LES of compressible flows [4].

The performance of standard explicit low-order finite-difference schemes in large-eddy simulations of turbulent flows is sometimes limited by the ability of these schemes to resolve high wavenumber modes. High resolution implicit finite-difference or spectral schemes are often used to avoid this problem. However, it is sometimes desirable to use explicit schemes, either because they are supported by existing software, or because they are efficient when implemented on parallel machines, for example. In that case, it is possible to use specially tuned explicit finite-difference schemes in which order of accuracy is sacrificed in favour of improved resolution at high wavenumber. Such schemes have been developed for collocated grids by Hill and Pullin [4], who constructed schemes that minimised the discretisation error in turbulent flows.

Standard finite-difference schemes have excellent resolution properties on staggered grids. However, when these are combined with the necessary interpolation schemes, the effective resolution properties are similar to those of standard finite-difference schemes on collocated grids [9].

The aim of this work is to develop and test tuned finite-difference and interpolation schemes for large-eddy simulation of incompressible turbulent flows on staggered grids using the stretched-vortex subgrid model. This is done by emulating the modified wavenumber behaviour of the tuned collocated schemes developed by Hill and Pullin [4].

Governing equations

The governing equations for large-eddy simulation of an incompressible flow are

$$\frac{\partial \overline{u}_j}{\partial x_j} = 0, \tag{1a}$$

$$\frac{\partial \overline{u}_i}{\partial t} + \frac{\partial \overline{u}_i \overline{u}_j}{\partial x_j} = -\frac{\partial \overline{p}/\rho}{\partial x_i} + \frac{\partial \overline{\tau}_{ij}}{\partial x_j} - \frac{\partial T_{ij}}{\partial x_j}, \tag{1b}$$

where x_i and u_i are the components of the Eulerian position and velocity vectors, respectively, p is the pressure, τ_{ij} is the viscous stress tensor given by

$$\tau_{ij} = \nu \left[\frac{\partial u_i}{\partial x_j} + \frac{\partial u_j}{\partial x_i} \right] \tag{2}$$

and ν is the kinematic viscosity. In the derivation of the governing equations, overbars denote the filtering operation

$$\overline{f} = \int G(x - x') f(x') \, \mathrm{d}x', \tag{3}$$

where G is a filter kernel. It is assumed that the filtered variables correspond to the resolved-scale quantities obtained in an actual LES. The additional term,

$$T_{ij} = \overline{u_i u_j} - \overline{u}_i \overline{u}_j, \tag{4}$$

is the subgrid stress.

The stretched-vortex subgrid stress model of Misra & Pullin [7] is used to close equation (1b). The subgrid stress is

$$T_{ij} = K(\delta_{ij} - e_i^v e_j^v) \tag{5}$$

where K is the subgrid kinetic energy per unit mass, and e_i^v are the components of a unit vector that is aligned with the subgrid vortex axis. The subgrid kinetic energy is

$$K = \int_{k_c}^{\infty} E(k) \, \mathrm{d}k, \tag{6}$$

where k is the wavenumber, $k_c = \pi/\Delta$ is the cut-off wavenumber, $E(k)$ is the spectrum of the Lundgren spiral vortex,

$$E(k) = \mathcal{K}_0 \varepsilon^{2/3} k^{-5/3} e^{-\lambda_v^2 k^2}, \tag{7}$$

$\mathcal{K}_0$ is the Kolmogorov prefactor, ε is the local cell-averaged dissipation rate, $\lambda_v^2 = 2\nu/(3|a|)$, $a = e_i^v e_j^v \overline{S}_{ij}$ is the axial strain along the subgrid vortex axis [11] and $\overline{S}_{ij}$ is the resolved rate-of-strain tensor. The parameters $\mathcal{K}_0 \varepsilon^{2/3}$ and a are calculating using procedures described by Mattner [6]. Subgrid vortices are assumed to align either with the principal extensional eigenvector of the resolved rate-of-strain tensor, $\overline{S}_{ij}$, or the resolved vorticity vector, ω, according to a model given by Kosovic, Pullin and Samtaney [5].
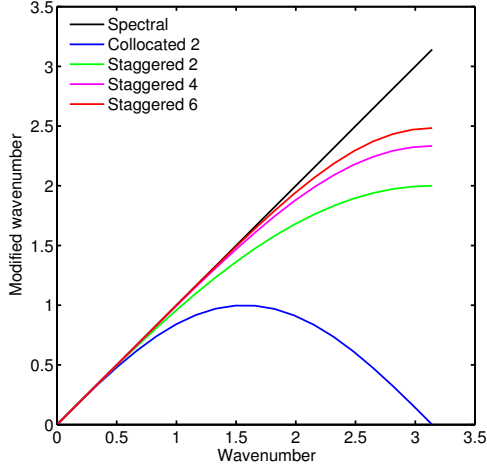
Figure 1: Modified wavenumber for standard staggered finite-difference schemes (14), (12) and (10) (Staggered 2, Staggered 4 and Staggered 6, respectively) and the standard second-order collocated finite difference scheme (Collocated 2).

Numerical methods

A conventional staggered grid arrangement is used in which the velocity components are located on cell faces and the pressure and other scalar variables are located at cell centres. The grid is uniformly spaced in each direction.

Explicit finite-difference schemes are used to discretise the derivatives in the governing equations. Staggered schemes for the first derivative are given by

$$f_j' = a\frac{f_{j+\frac{1}{2}} - f_{j-\frac{1}{2}}}{\Delta} + b\frac{f_{j+\frac{3}{2}} - f_{j-\frac{3}{2}}}{3\Delta} + c\frac{f_{j+\frac{5}{2}} - f_{j-\frac{5}{2}}}{5\Delta}, \quad (8)$$

where $f_j = f(x_j)$, $x_j = j\Delta$, Δ is the grid spacing, a, b and c are coefficients and $f_j' \approx f'(x_j)$. Eliminating successively higher order terms in the Taylor series about x_j yields

$$a + b + c = 1 \quad \text{at } O(\Delta^2), \quad (9a)$$

$$a + 9b + 25c = 0 \quad \text{at } O(\Delta^4), \quad (9b)$$

$$a + 81b + 625c = 0 \quad \text{at } O(\Delta^6). \quad (9c)$$

Satisfying all three equations yields the sixth-order accurate schemes whose coefficients are

$$a = \frac{150}{128}, \quad b = -\frac{25}{128}, \quad c = \frac{3}{128}. \quad (10)$$

Ignoring (9c) yields a single-parameter family of fourth-order accurate schemes,

$$a = \frac{9}{8} + 2c, \quad b = -\frac{1}{8} - 3c. \quad (11)$$

This includes the standard fourth-order accurate scheme given by

$$a = \frac{9}{8}, \quad b = -\frac{1}{8}, \quad c = 0. \quad (12)$$

Ignoring (9b) and (9c) yields a two-parameter family of second-order accurate schemes,

$$a = 1 - b - c. \quad (13)$$

This includes the standard second-order accurate scheme given by

$$a = 1, \quad b = 0, \quad c = 0. \quad (14)$$
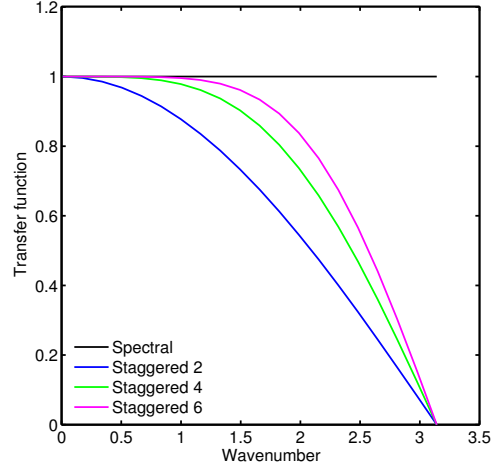
Figure 2: Transfer functions for interpolation schemes (14), (12) and (10) (Staggered 2, Staggered 4 and Staggered 6, respectively).

Explicit interpolation schemes are used to to interpolate from cell faces or vertices to cell centres and vice versa. These schemes are given by

$$\tilde{f}_j = \alpha\frac{f_{j+\frac{1}{2}} + f_{j-\frac{1}{2}}}{2} + \beta\frac{f_{j+\frac{3}{2}} + f_{j-\frac{3}{2}}}{2} + \gamma\frac{f_{j+\frac{5}{2}} + f_{j-\frac{5}{2}}}{2}, \quad (15)$$

Eliminating successively higher order terms in the Taylor series about x_j yields a system of equations that is analogous to (9), except that a, b and c are replaced by α, β and γ, respectively. Consequently, families of interpolation schemes of varying accuracy can be constructed in the same way as (10) through to (14).

Fourier analysis is used to quantify the resolution of these numerical differentiation and interpolation schemes. Consider a 2π periodic function of the form

$$f(x) = \sum_{k=-N/2}^{N/2-1} \hat{f}_k e^{ikx},$$

where N is the number of grid points and $\hat{f}_k$ is the Fourier coefficient corresponding to wavenumber k. The Fourier coefficient of the staggered finite-difference approximation of the derivative (8) is $ik'(k)\hat{f}_k$, where $k'(k)$ is the modified wavenumber given by

$$k'(k)\Delta = 2a\sin\left(\frac{k\Delta}{2}\right) + \frac{2b}{3}\sin\left(\frac{3k\Delta}{2}\right) + \frac{2c}{5}\sin\left(\frac{5k\Delta}{2}\right). \quad (16)$$

For spectral differentiation, $k' = k$. The Fourier coefficient of the interpolated function represented by (8) is $T(k)\hat{f}_k$, where $T(k)$ is the transfer function given by

$$T(k) = \alpha\cos\left(\frac{k\Delta}{2}\right) + \beta\cos\left(\frac{3k\Delta}{2}\right) + \gamma\cos\left(\frac{5k\Delta}{2}\right). \quad (17)$$

For spectral schemes, $T(k) = 1$.

Staggered finite-difference schemes have excellent resolution properties when compared to those of explicit collocated schemes. Figure 1 shows the modified wavenumber of the standard second-, fourth- and sixth-order staggered finite-difference schemes, as well as that of the standard second-order collocated scheme $f_j' = (f_{j+1} - f_{j-1})/(2\Delta)$. The staggered second-order
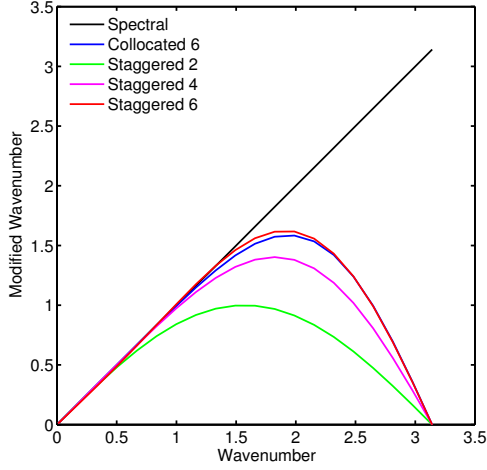
Figure 3: Modified wavenumber of $\tilde{f}'_j$ for standard staggered schemes (14), (12) and (10), (Staggered 2, Staggered 4 and Staggered 6, respectively) compared with that of the standard sixth-order collocated scheme. (Collocated 6)

Figure 4: Modified wavenumber of $\tilde{f}'_j$ for the second and fourth-order tuned staggered schemes (Staggered 2T, Staggered 4T), fourth and sixth-order standard staggered schemes (Staggered 4, Staggered 6) and second and fourth-order tuned collocated schemes of Hill & Pullin [4].

scheme is clearly better at resolving high wavenumber modes than the second-order collocated scheme.

Interpolation is used for evaluating the nonlinear and subgrid stress terms in the governing equations (1) and this affects the overall resolution. Figure 2 shows the transfer functions of the standard second-, fourth- and sixth-order interpolation schemes. Interpolation clearly attenuates the high wavenumber modes, especially for the lower-order schemes.

The resolution of the composite staggered-grid finite-difference and interpolation scheme is assessed by calculating the modified wavenumber of $\tilde{f}'_j$, which is

$$
\begin{aligned}
k'(k)\Delta = {} & \left[a(\alpha - \beta) + \frac{b(\alpha - \gamma)}{3} + \frac{c\beta}{5} \right] \sin k\Delta \\
& + \left[a(\beta - \gamma) + \frac{\alpha b}{3} + \frac{\alpha c)}{5} \right] \sin 2k\Delta \\
& + \left[a\gamma + \frac{b\beta}{3} + \frac{c\alpha}{5} \right] \sin 3k\Delta \\
& + \left[\frac{b\gamma}{3} + \frac{c\beta}{5} \right] \sin 4k\Delta + \frac{c\gamma}{5} \sin 5k\Delta. \quad (18)
\end{aligned}
$$

Although the full details of the implementation of the nonlinear and subgrid stress terms are ignored, this simplified approach is nevertheless useful for comparing the resolution of staggered schemes with their collocated counterparts [9]. Figure 3 shows the modified wavenumber of the composite second-, fourth- and sixth-order staggered schemes, as well as that of the standard sixth-order collocated scheme. The resolution of these composite schemes is very similar to that of standard collocated schemes for the same order of accuracy.

Tuned schemes are obtained by sacrificing order of accuracy in favour of improved modified wavenumber performance for a given stencil. A tuned second-order staggered finite-difference scheme with a four-point stencil is obtained by setting $c = 0$ and using b in (13) as the tuning parameter. Likewise, a tuned second-order interpolation operator is obtained by setting $\gamma = 0$ and using β as the tuning parameter. Tuned fourth-order staggered finite-difference and interpolation operators with a six-point stencil are obtained by using c in (11) and γ as tuning parameters. In this exploratory study, the tuning parameters are adjusted so that the modified wavenumber of the compos-

ite scheme is similar that of the collocated schemes obtained by Hill & Pullin [4]. The tuned second-order schemes used here are given by
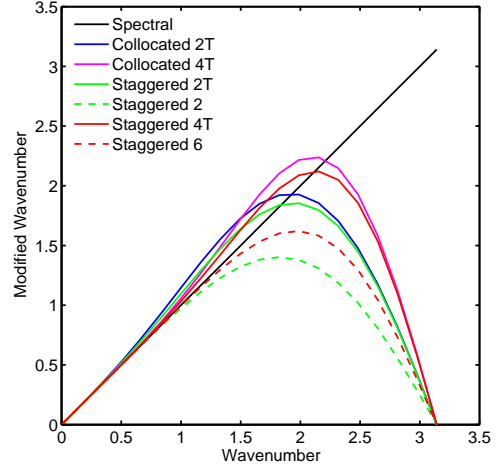
$$
\begin{aligned}
a &= 1.27, \quad b = -0.27, \quad c = 0, \\
\alpha &= 1.22, \quad \beta = -0.22, \quad \gamma = 0. \quad (19)
\end{aligned}
$$

The tuned fourth-order schemes used here are given by

$$
\begin{aligned}
a &= 1.295, \quad b = -0.38, \quad c = 0.085, \\
\alpha &= 1.245, \quad \beta = -0.305, \quad \gamma = 0.06. \quad (20)
\end{aligned}
$$

Figure 4 shows the modified wavenumber of the tuned composite schemes, together with the tuned collocated schemes obtained by Hill & Pullin [4] and the standard fourth and sixth-order composite schemes. For this choice of parameters, the modified wavenumber behaviour of the tuned composite schemes is similar to that of the tuned collocated schemes.

A third-order low-storage Runge–Kutta scheme is used for temporal integration. A Poisson equation for the pressure is solved at each substep in order to enforce the incompressibility constraint (1a). The nonlinear terms are evaluated using the skew-symmetric form in order to minimise aliasing. The subgrid model is evaluated at cell-centres by interpolating components of the velocity and velocity gradient tensor to the cell centres.

Results and discussion

The results presented here are obtained from simulations of three-dimensional decaying homogeneous isotropic turbulence using the stretched-vortex model with the standard second, fourth and sixth-order staggered finite-difference and interpolation schemes, as well as the second and fourth-order tuned staggered finite-difference and interpolation schemes. All simulations were run in a triply-periodic domain using 32^3 grid points. The initial velocity field was solenoidal, with a spectrum of the form

$$
A \left(\frac{k}{k_0} \right)^4 \exp \left[-2 \left(\frac{k}{k_0} \right)^2 \right],
$$

where A is an amplitude and $k_0/k_c = 1/4$, and randomly generated phase angles. The initial Reynolds number was $Re_\lambda = $
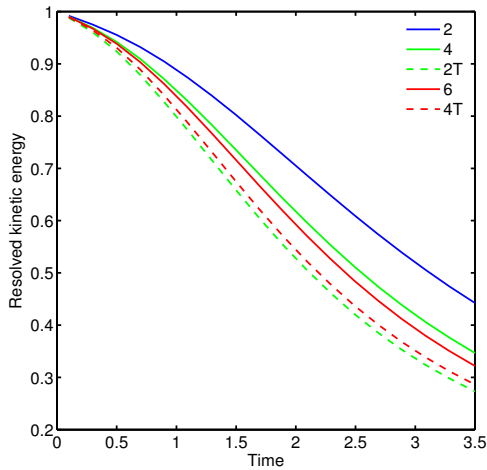
Figure 5: Resolved turbulent kinetic energy for standard second, fourth and sixth-order staggered schemes (2, 4 and 6, respectively) and second and fourth-order tuned staggered schemes (2T and 4T, respectively).

Figure 6: Resolved turbulent kinetic energy spectrum for standard second, fourth and sixth-order staggered schemes (2, 4 and 6, respectively) and second and fourth-order tuned staggered schemes (2T and 4T, respectively). The slope of the black line is $-5/3$.

$u'\lambda/\nu = 1000$, where u' is the root-mean-square velocity fluctuation and λ is the Taylor microscale.

Figure 5 shows the evolution of the resolved tubulent kinetic energy normalised by its intial value. There is a considerable difference between the standard second-order scheme and the other standard schemes. The standard fourth and sixth-order schemes are more consistent, as are the tuned second and fourth-order schemes, but there is a noticeable gap between the standard and tuned schemes.

Figure 6 shows the shell-summed energy spectrum at time $t = 1$. Once again, there is a sizeable difference between the standard second-order scheme and the other schemes, with a smaller difference between the fourth and sixth-order standard schemes and the tuned schemes. By $t = 1$, the tuned schemes produce spectra with a slope that is close to $-5/3$, except at the highest resolved wavenumbers, where there is a distinctive upturn. Somewhat smaller upturns are evident in the spectra presented by Hill, Pantano and Pullin [3], where they are attributed to aliasing.

These results support previous conclusions [e.g. 5, 4] that large-eddy simulations using the stretched-vortex model are sensitive to numerical discretisation. It is encouraging that the tuned schemes produce self-consistent results, as this suggests that the tuned schemes are adequately resolving the flow. Comparison with a spectral calculation and inclusion of subgrid-scale contributions to the statistics would be more conclusive.

Conclusions

The explicit tuned staggered finite-difference and interpolation schemes used in this study emulate the modified wavenumber behaviour of collocated schemes that minimise the discretisation error in a large-eddy simulation. These schemes lead to self-consistent simulations of isotropic homogeneous turbulence on a staggered grid.

*

References

[1] Chung, D. and Pullin, D. I., Large-eddy simulation and wall modelling of turbulent channel flow, *J. Fluid Mech.*, **631**, 2009, 281–309.
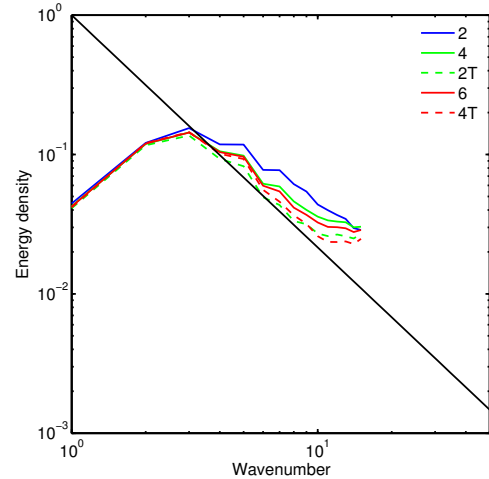
[2] Chung, D. and Pullin, D. I., Direct numerical simulation and large-eddy simulation of stationary buoyancy-driven turbulence, *J. Fluid Mech.*, **643**, 2010, 279–308.

[3] Hill, D. J., Pantano, C. and Pullin, D. I., Large-eddy simulation and multiscale modelling of a Richtmyer-Meshkov instability with reshock, *J. Fluid Mech.*, **557**, 2006, 29–61.

[4] Hill, D. J. and Pullin, D. I., Hybrid tuned center-difference–WENO method for large eddy simulations in the presence of strong shocks, *J. Comp. Phys.*, **194**, 2004, 435–450.

[5] Kosovic, B., Pullin, D. I. and Samtaney, R., Subgrid-scale modeling for large-eddy simulations of compressible turbulence, *Phys. Fluids*, **14**, 2002, 1511–1522.

[6] Mattner, T. W., A refined stretched-vortex model for large-eddy simulation of turbulent mixing layers, in *17th Australasian Fluid Mechanics Conference*, Auckland, New Zealand, 2010.

[7] Misra, A. and Pullin, D. I., A vortex-based subgrid stress model for large-eddy simulation, *Phys. Fluids*, **9**, 1997, 2443–2454.

[8] Morinishi, Y., Lund, T. S., Vasilyev, O. V. and Moin, P., Fully conservative higher order finite difference schemes for incompressible flow, *J. Comp. Phys.*, **143**, 1998, 90–124.

[9] Nagarajan, N., Lele, S. K. and Ferziger, J. H., A robust high-order compact method for large eddy simulation, *J. Comp. Phys.*, **191**, 2003, 392–419.

[10] Pullin, D. I., A vortex-based model for the subgrid flux of a passive scalar, *Phys. Fluids*, **12**, 2000, 2311–2319.

[11] Voekl, T., Pullin, D. I. and Chan, D. C., A physical-space version of the stretched-vortex subgrid-stress model for large-eddy simulation, *Phys. Fluids*, **12**, 2000, 1810–1825.